Supplement of Nat. Hazards Earth Syst. Sci., 22, 1347–1369, 2022
https://doi.org/10.5194/nhess-22-1347-2022-supplement

Natural Hazards and Earth System Sciences
Open Access
EGU

Supplement of

Hotspots for warm and dry summers in Romania

Viorica Nagavciuc et al.

Correspondence to: Monica Ionita (monica.ionita@awi.de)

Table S1. Results of the trend analysis for HWDI (Figure 2 – left column). The trend analysis was conducted based on nonparametric Mann-Kendall test. The analysis was performed over the period 1951 – 2020.

		HWDI Trend	P-value
June	E-OBS	0.52 days/decade	3.37E-5*
July	E-OBS	0.31 days/decade	0.0014*
August	E-OBS	0.43 days/decade	0.0022*
JJA	E-OBS	1.2 days/decade	5.23E-4*

The null hypothesis of no trend is rejected if the p-values is lower than 0.05 (significance level of α =0.05).
* indicates a statistically significant trend the 90% confidence level using the Mann–Kendall test.

Table S2. Results of the trend analysis for the monthly SPEI (Figure5 – left column). The trend analysis was conducted based on nonparametric Mann-Kendall test. The analysis was performed over the period 1951 – 2020.

		SPI Trend	P-value
June SPEI1	E-OBS	-0.002 z-scores/decade	0.626
July SPEI1	E-OBS	-0.004 z-scores/decade	0.488
August SPEI1	E-OBS	-0.011 z-scores/decade	0.045*
August SPEI3	E-OBS	-0.008 z-scores/decade	0.135

The null hypothesis of no trend is rejected if the p-values is lower than 0.05 (significance level of α =0.05).
* indicates a statistically significant trend the 90% confidence level using the Mann–Kendall test.

Table S3. Results of the trend analysis for the monthly Z500 indices (Figure 13 – right column). The trend analysis was conducted based on nonparametric Mann-Kendall test, for two distinct period: 1950 – 2020 and 1990 - 2020.

		Z500 Index Trend	P-value
June	1950 – 2020	2.8m/decade	0.06
	1990 – 2020	12.5m/decade	0.005*
July	1950 – 2020	2.8m/decade	0.009*
	1990 – 2020	7.5m/decade	0.001*
August	1950 – 2020	4.3m/decade	0.0007*
	1990 – 2020	11.5m/decade	0.006*

The null hypothesis of no trend is rejected if the p-values is lower than 0.05 (significance level of α =0.05).
* indicates a statistically significant trend the 90% confidence level using the Mann–Kendall test.

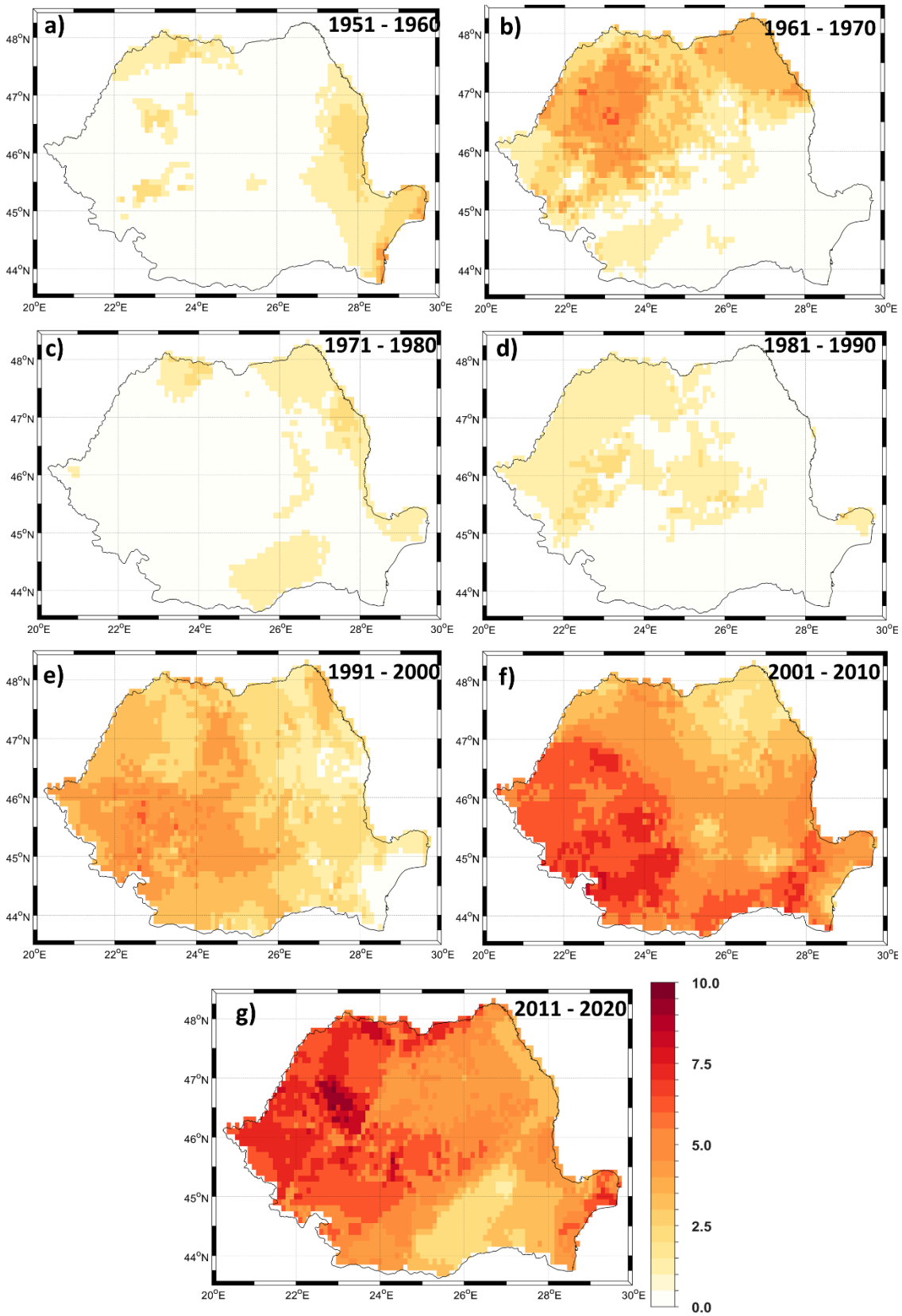

Figure S1. June decadal frequency of the number of heat waves (HWs) per decade over the last 70 years: a) 1951 – 1960; b) 1961 – 1970; c) 1971 – 1980; d) 1981 – 1990; e) 1991 – 2000; f) 2001 – 2010 and g) 2011 – 2020. Units: number of HWs/decade.

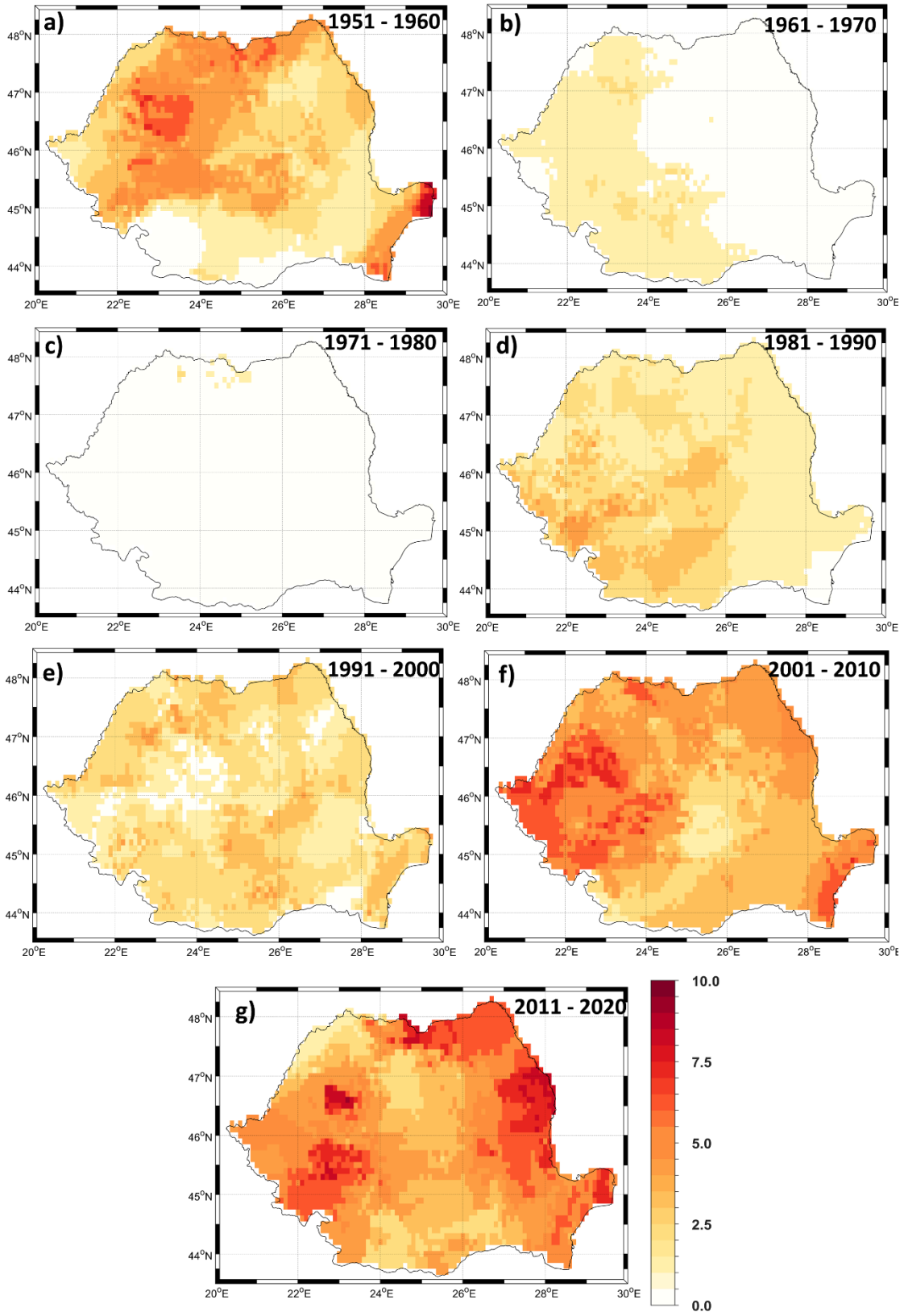

Figure S2. July decadal frequency of the number of heat waves (HWs) per decade over the last 70 years: a) 1951 – 1960; b) 1961 – 1970; c) 1971 – 1980; d) 1981 – 1990; e) 1991 – 2000; f) 2001 – 2010 and g) 2011 – 2020. Units: number of HWs/decade.

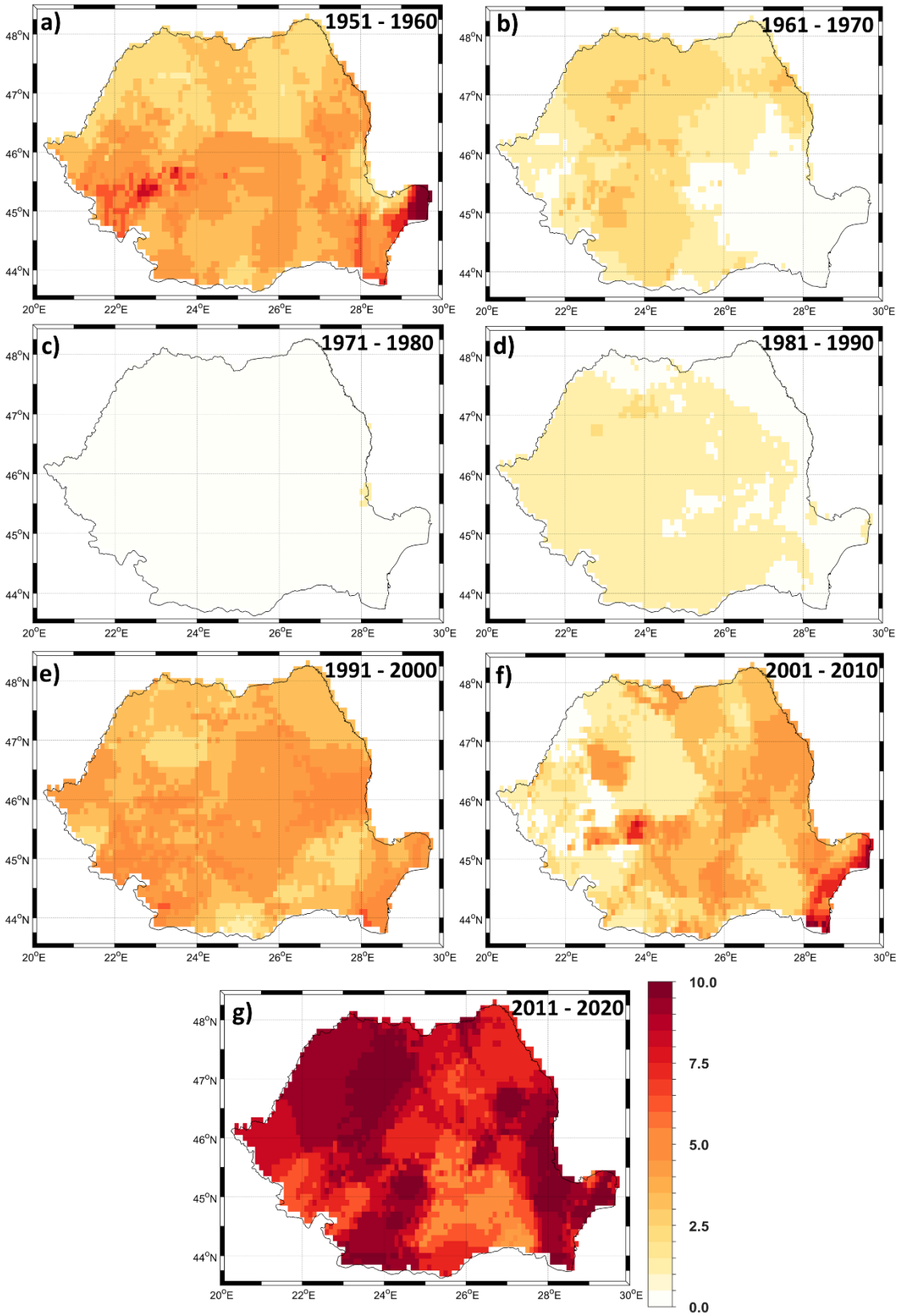

Figure S3. August decadal frequency of the number of heat waves (HWs) per decade over the last 70 years: a) 1951 – 1960; b) 1961 – 1970; c) 1971 – 1980; d) 1981 – 1990; e) 1991 – 2000; f) 2001 – 2010 and g) 2011 – 2020. Units: number of HWs/decade.

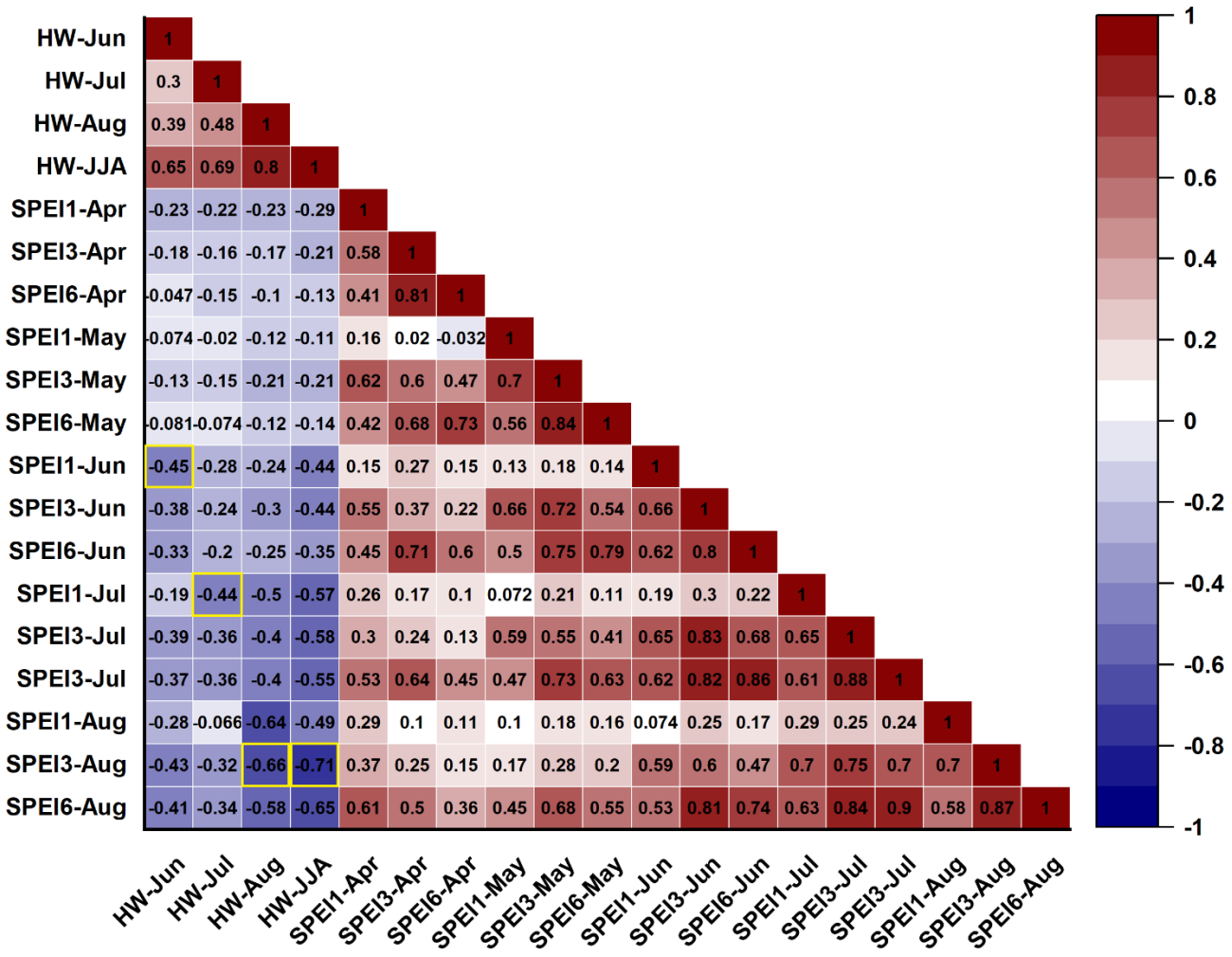

Figure S4. The correlation coefficient between the monthly SPEI and monthly HWDI with different time lags and in phase. The combinations (SPEI and HWDI) which are used in the study to compute the compund hot and dry (CHD) index are highlighted in yellow boxes.

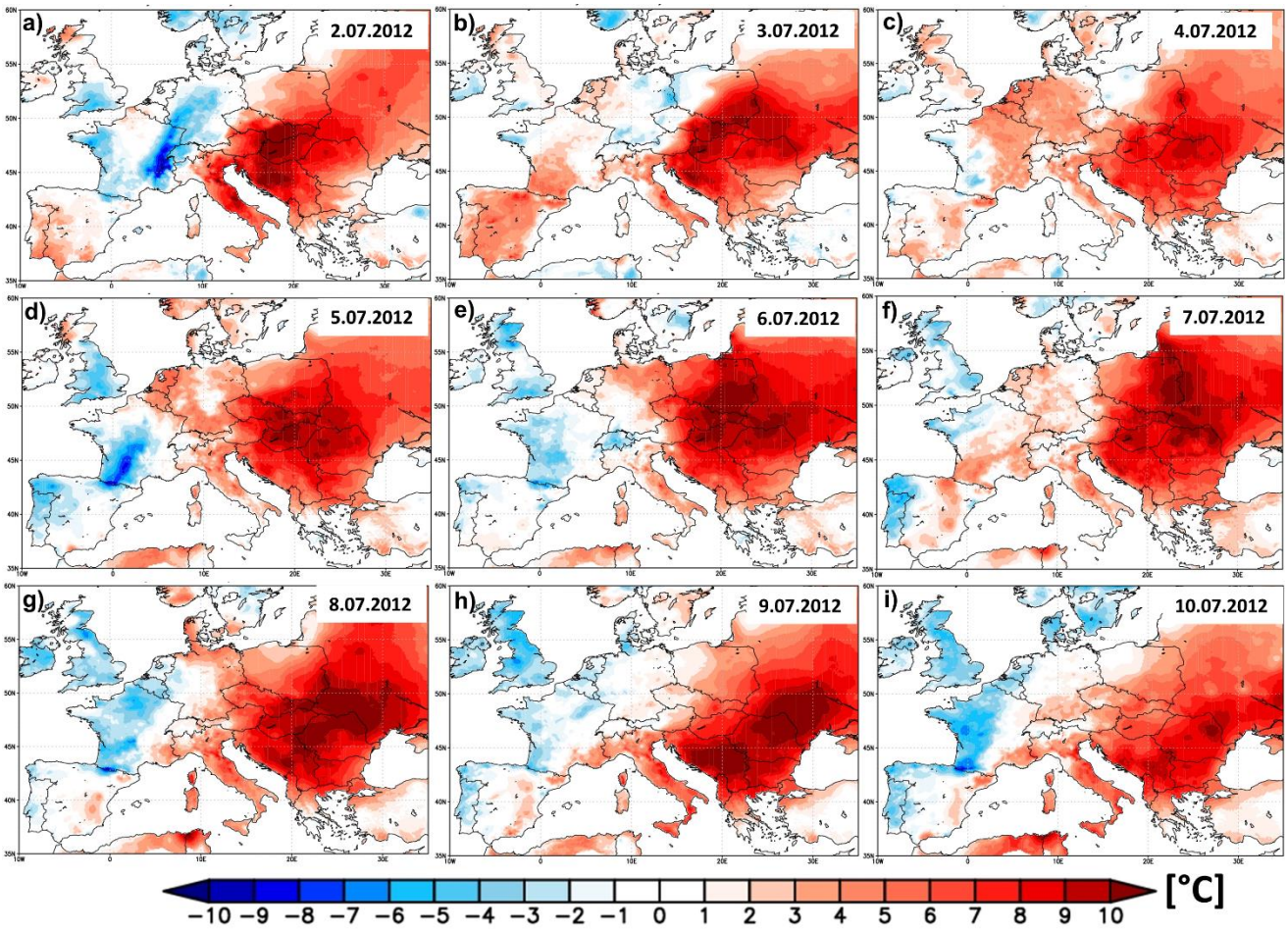

Figure S5. Evolution of the daily maximum temperature (Tx) anomaly over the period 2.07.2012 – 10.07.2012. The anomalies are computed relative to the base period 1971 – 2000.

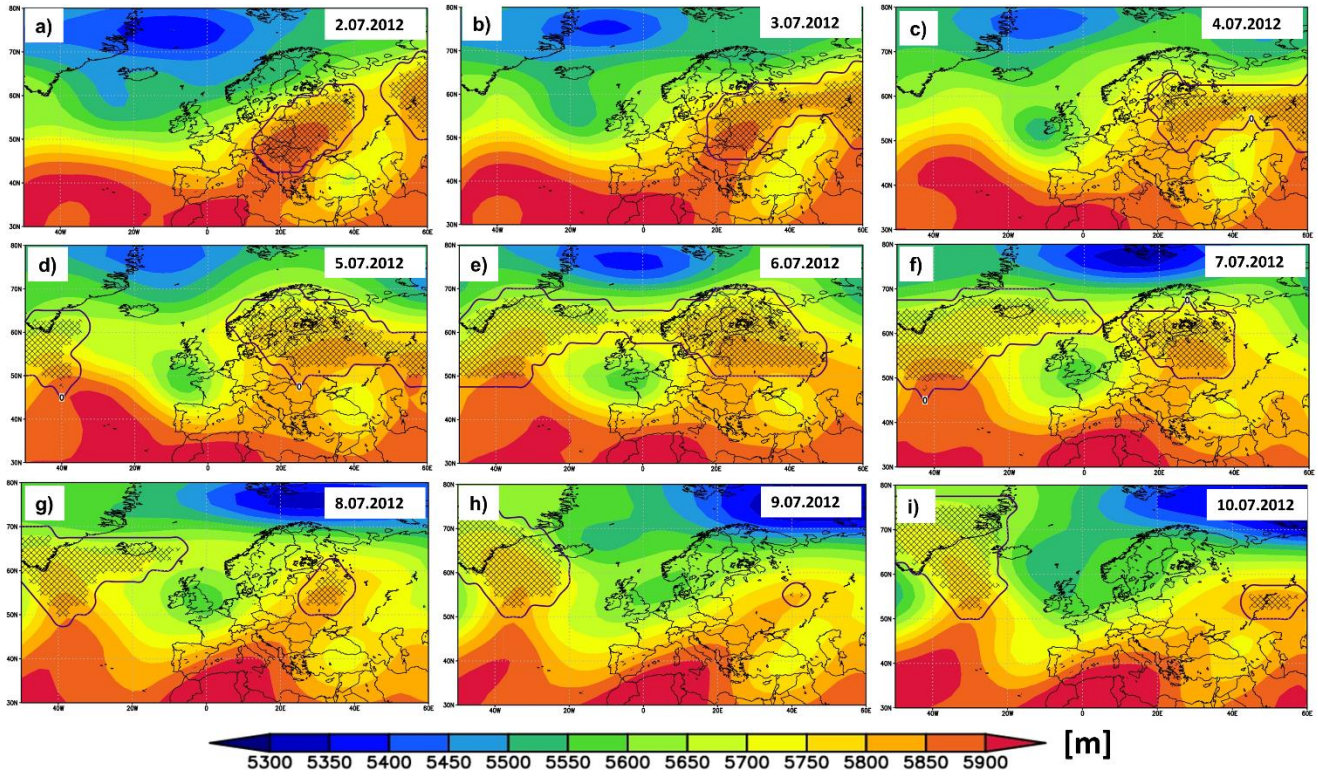

Figure S6. Evolution of the daily geopotential height at 500mb (shaded colors) and the location of the 2D atmospheric blocking (contour lines and hashed areas) over the period 2.07.2012 – 10.07.2012.

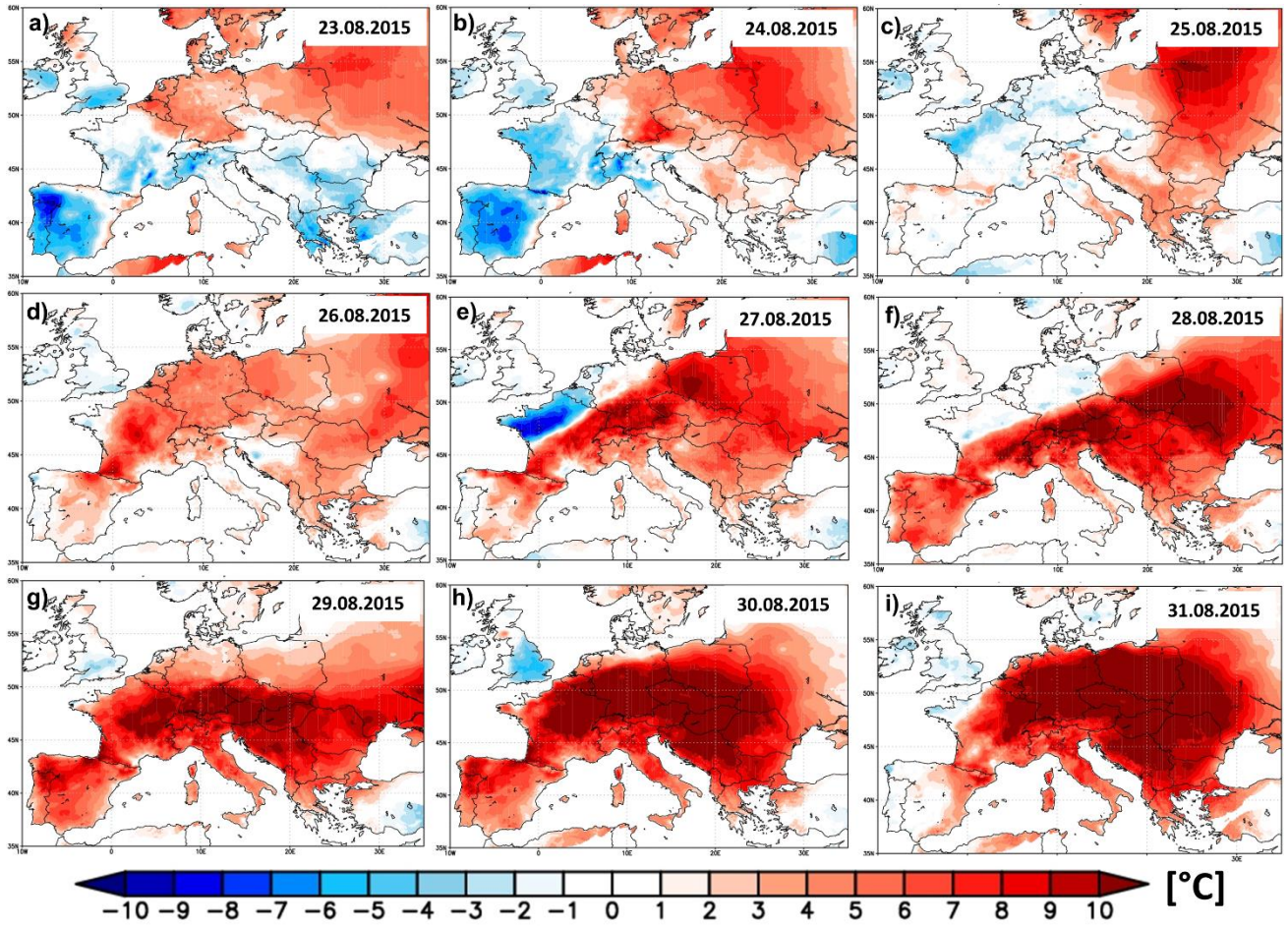

Figure S7. Evolution of the daily maximum temperature (Tx) anomaly over the period 23.08.2015 – 31.08.2015. The anomalies are compute relative to the base period 1971 – 2000.

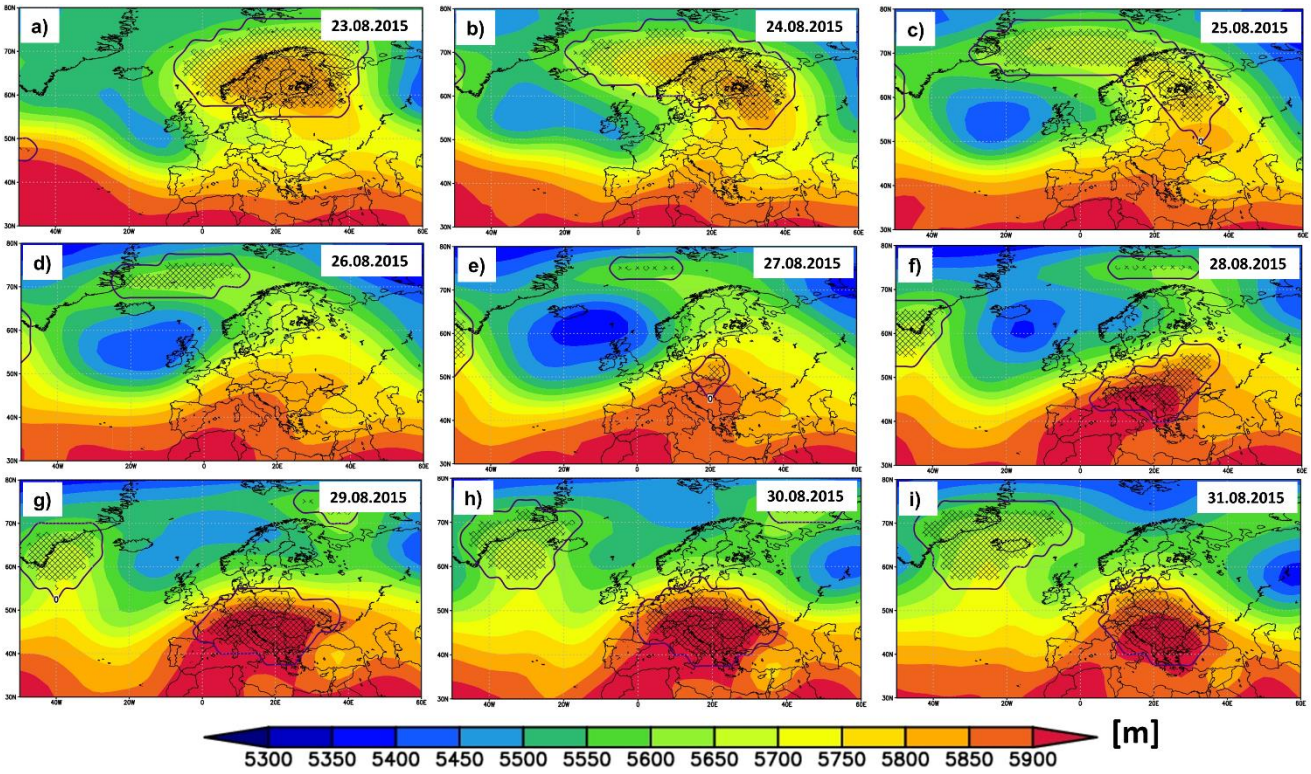

Figure S8. Evolution of the daily geopotential height at 500mb (shaded colors) and the location of the 2D atmospheric blocking (contour lines and hashed areas) over the period 23.078.2015 – 31.08.2015.

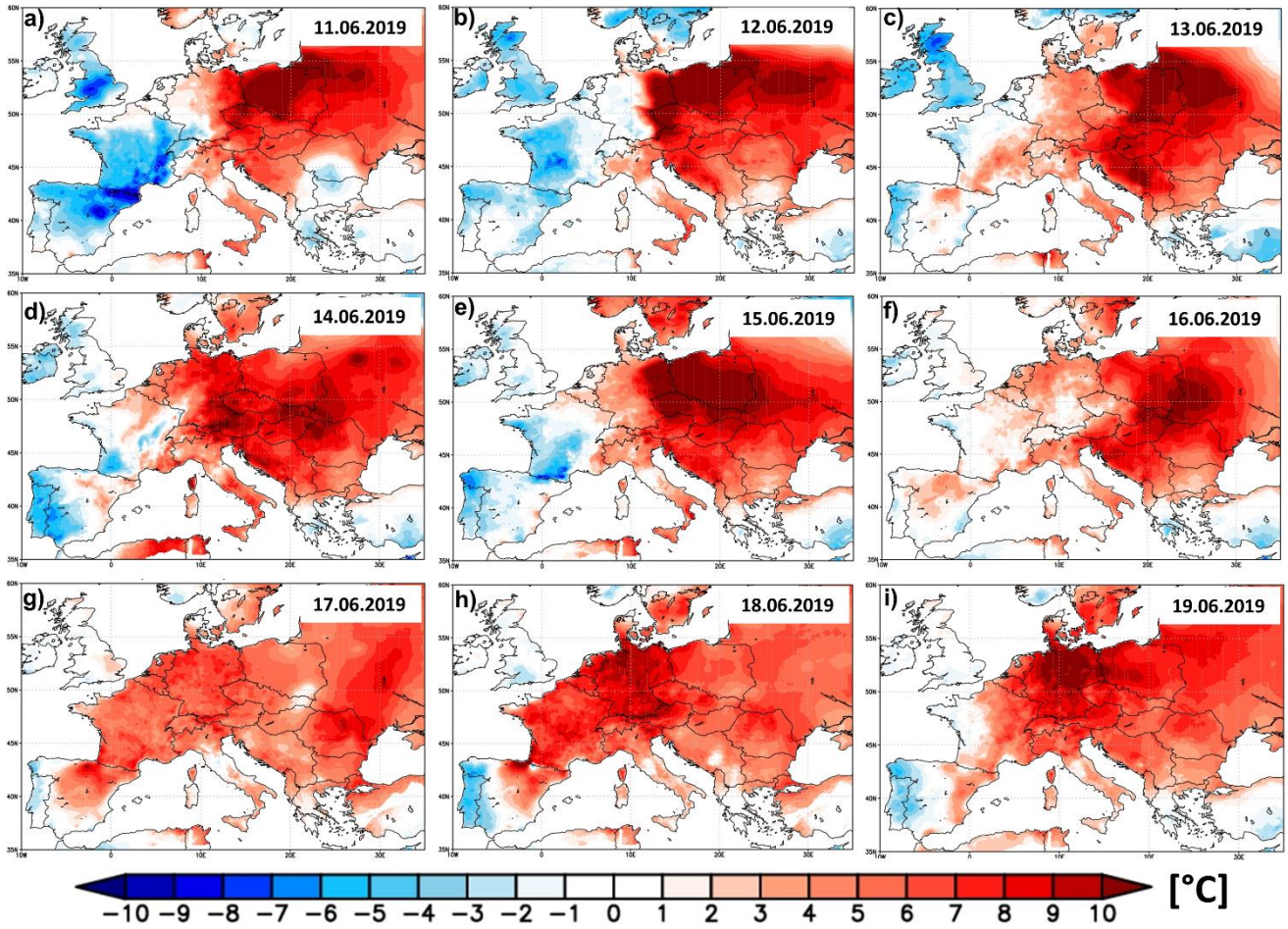

Figure S9. Evolution of the daily maximum temperature (Tx) anomaly over the period 11.06.2019 – 19.06.2019. The anomalies are compute relative to the base period 1971 – 2000.

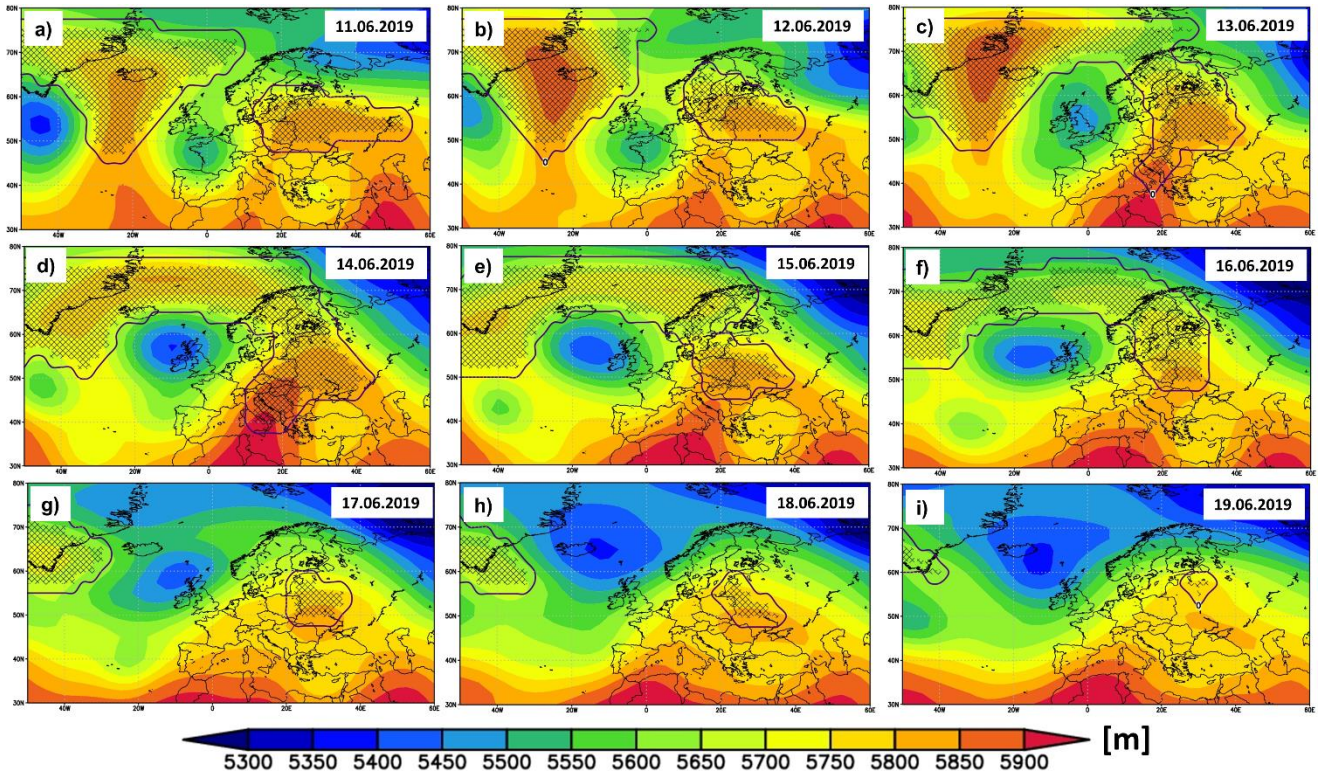

Figure S10. Evolution of the daily geopotential height at 500mb (shaded colors) and the location of the 2D atmospheric blocking (contour lines and hashed areas) over the period 11.06.2019 – 19.06.2019.